Indian Journal of Engineering & Materials Sciences
Vol. 27, October 2020, pp. 976-983

Ultra-violet responsive photocatalytic application of CuO/Bi oxide nitrate hydroxide hydrate powder

Miljana Radović Vučić*, Jelena Mitrović, Miloš Kostić, Nena Velinov, Milica Petrović, Danijela Bojić & Aleksandar Bojić

The University of Niš, Faculty of Sciences and Mathematics, Višegraska 33, 18000 Niš, Serbia

Received: 26 September 2019; Accepted: 28 May 2020

A new photocatalyst CuO/Bi oxide nitrate hydroxide hydrate (C-BONH) has been synthesized by hydrothermal method. The obtained product has been characterized using x-rays diffraction (XRD), fourier transform infrared spectroscopy (FTIR), scanning electron microscopy (SEM) and energy-dispersive X-ray spectroscopy (EDS). The surface area has been measured by Brunauer-Emmett-Teller (BET) method, and it has been found 4.42 m^2 g^{-1}. The photocatalytic activity has been evaluated by removal of reactive blue 19 (RB 19) dye, where total decolorization has been achieved in less than 15 minutes. The photocatalytic process is described with four kinetic models (Langmuir–Hinshelwood model, pseudo-first order kinetic model, pseudo-second order kinetic model and Chrastil diffusion model). Langmuir–Hinshelwood kinetic model and pseudo-first order kinetic model the best describe the photocatalytic process. Chrastil diffusion model has been shown that diffusion has not any influence on the process. The chemical oxygen demand (COD) has been decreased from 28.1 to 6.82 mg dm^{-3}within 180 minusing UV light (254 nm wavelength). It has been observed that photocatalyst retained its stability and activity even after five cycles, which could significantly reduce the operation cost in practical applications.

Keywords: Photocatalyst, Ultra-violet light irradiation**,** Reactive blue 19, Decolorization, Kinetics

1 Introduction

In recent years, approximately 12-20% of synthetic dyes have been frequently used in textile industries to color cotton, woollen and polyamide fibers. The presence of organic pollutants such as reactive textile dyes in water resources is a serious threat to the public health and environment due to their high water solubility, low biodegradability and high toxicity[1].

In the past decades, some techniques such as biological treatments, sorption, membrane separation, coagulation, chemical oxidation,electrochemical technology, and advanced oxidation processes have been investigated to treat dyeing wastewater. However, low removal efficiency or high cost in operation often limit their application[2].

Among them, heterogeneous photocatalytic processes frequently used because of its high efficiency, economic feasibility, and operational simplicity.The main advantage of heterogeneous photocatalysis is the ability of the totalmineralization of dyes, resulting in the formation of CO_2,H_2O, and the corresponding mineral matter, leaving no waste forsecond disposal[3,4]. An important driving force for the growing interest in these environmentally relevant applications of bismuth is the relatively low toxicity of bismuth compounds as compared to related species containing heavy metals such as Hg, In, Cd, Sn or Pb. Other advantages of heterogeneous photocatalysis are that it does not require using any other chemicals or soluble catalysts, except insoluble photocatalyst, which can be recovered and re-used, so that secondary pollution is not formed. Bismuth-contained materials are taken into account due to its cheapness and the innocuity.Developing a new efficient photocatalyst is still a great challenge in the photocatalysis field so far.

In recent years, nanomaterials based on bismuth compounds, as a new family of promising photocatalysts have attracted increasing interest in heterogeneous photocatalysis[5–12].

In this study, a process of synthesis, characterization, and application of a novel CuO/Bi oxide nitrate hydroxide hydrate (C-BONH) catalyst was studied. A simple hydrothermal procedure at a temperature of 120 ºC was applied for the synthesis. Also the applied hydrothermal procedure does not require rigorous synthetic conditions. The structural characterizations of C-BONH have been performed through different techniques such as: Brunauer-Emmett-Teller (BET) method, x-rays diffraction (XRD), fourier transform infrared

*Corresponding authors: (E-mail:mimaradovic@gmail.com)

spectroscopy (FTIR) to confirm the formation of nanopowder, scanning electron microscopy (SEM) and energy-dispersive X-ray spectroscopy (EDS) to explore the surface morphology, size of the particles and elemental composition. Moreover, the photocatalytic activities of hydrothermal sample for degradation of aanthraquinone reactive dye Reactive Blue 19 (RB 19)was examined. Bismuth-based photocatalyst show high activity and good catalytic stability.The effect of different variables, including pH, temperature, catalyst dose, contact time and initial dye concentration was evaluated. Kinetics and diffusion models, as well as durability, were all examined for a better understanding of the photocatalytic process.

2 Experimental

2.1 Materials and reagents

The anthraquinone reactive dye C.I. Reactive Blue 19 (RB 19) (Mw = 626.55 g mol^{-1}) was obtained from Sigma-Aldrich (USA) and used without any purification. $Bi(NO_3)_3$ x $5H_2O$, $Cu(CH_3COO)_2$, ethanol, HNO_3 and NaOH were of analytical grade and purchased from Merck (Germany). All solutions were prepared with deionized water (18 MΩ).

2.2 Preparation of catalyst

The C-BONH photocatalyst was made by hydrothermal method using bismuth-nitrate pentahydrate [$Bi(NO_3)_3 \cdot 5\ H_2O$] as a precursor. The appropriate amount of $Bi(NO_3)_3 \cdot 5\ H_2O$ (4,2657 g) was dissolved and stirred to obtain a clear solution. Then, $(CH_3COO)_2Cu$ (0,6537 g) was added, pH was adjusted at 3 using NaOH, and the solution was magnetically stirred. The above solution was then transferred to autoclave. Subsequently, the autoclave was sealed and maintained at 120 ºC for 6 h. After the autoclave was cooled down to room temperature, products were collected by centrifugation, washed for 3 times with distilled water and absolute ethanol, and then dried at 80 ºC for 6h. After that, the photocatalyst was cooled to room temperature and ready to use.

2.3 Characterization of C-BONH

The infrared spectrum of C-BONHwas obtained by using a Fourier transform infrared spectrometer (Bomem Hartmann & Braun MB-100 spectrometer). The surface morphology of the C-BONH surface was analyzed by SEM (Hitachi SU8030). EDS analysis (Thermo Scientific NORAN System 7, USA) provides elemental information via the analysis of X-ray emissions from the catalyst surface. The crystal structure was analyzed by XRD using filtered Cu Kα radiation (Ultima IV Rigaku). The experiments were performed in the scan range 2θ = 5–90° under 40 kV, 40 mA, with scan speed 5 degrees/min and steps with 0.02°. Prior to the measurement, the angular correction was done by a high-quality Si standard.The specific surface area was measured by nitrogen adsorption using the Micromeritics Gemini 5 Surface Area Analyzer, USA. The specific surface area was determined using the Brunauer–Emmett-Teller (BET) method[13]. The Barret–Joyner–Halenda (BJH) method was used for pore volume, area, and diameter analysis[14].

2.4 Experimental set-up and procedure

A stock solution of RB 19 was made by dissolving 1.0 g dye in 1000.0 cm^{-3} of deionized water. Working solutions were prepared freshly, before irradiation, by diluting the stock to the desired concentration with deionized water. The pH of solutions was adjusted by addition of NaOH or HNO_3 (0.1/0.01 mol dm^{-3}). The suspensions of dye and C-BONH were magnetically stirred in dark for 30 min to attain adsorption-desorption equilibrium between dye and C-BONH, and then the dye solutions were treated in the UV reactor.

2.4.1 UV studies

Photochemical experiments were carried out in a batch photoreactor handmade in our laboratory (Fig. S1 in Supplementary material section). The UV lamps were turned on for 10 min before performing each experiment. The intensity of UV radiation was measured by a UV radiometer Solarmetermodel 8.0 UVC (Solartech, USA). The total UV intensity was controlled by turning on different numbers of UV lamps and the maximum intensity was 1950 μW cm^{-2} (with all ten UV lamps on) at the distance of 220 mm, from working solution surface.

The suspensions of dye and photocatalystwere magnetically stirred in dark for 30 min to attain adsorption-desorption equilibrium between dye and photocatalyst, and then the dye solutions are treated in the UV reactor. During irradiation, the solution was magnetically stirred (Are, Velp Scientifica, Italy) at a constant rate and temperature was maintained at 25 ± 0.5ºC by thermostating. At required time intervals, 4.0cm^{-3} of samples were withdrawn, centrifuged (3000 rpm, 5 min) and filtered through a 0.20 μm regenerated cellulose membrane filter (Agilent Technologies, Germany) to separate the catalyst. The remaining concentration of RB 19 was

determined by the UV-vis spectrophotometer. The removal (%) of RB 19 dye was calculated as:

$$\text{Removal (\%)} = \left[1 - \frac{C_t}{C_0}\right] \times 100 \quad \ldots (1)$$

where c_0 and c_t are the concentration values of the dye solution before and after UV irradiation respectively.

All the experiments were conducted in triplicate and average values were used in the data analysis using OriginPro 9.0 software (Origin Lab Corporation, USA).

2.4.2 Analysis

Absorbance at 592 nm was measured using a UV-vis spectrophotometer Shimadzu UV-1800 PC (Shimadzu, Japan) Shimadzu, Japan), after filtration through a 0.20 µm membrane filter (Agilent Technologies, Germany), to determine the degree of decolorization of the solution. A pH/ISE meter (Orion Star A214, Thermo scientific, USA) was used for pH measurements.

Chemical oxygen demand (COD) was measured by COD LR method with vario tube test method (Thermoreactor AL125, Aqualytic, Germany and Photometer-System AL450, Aqualytic, Germany).

2.5 Catalyst reuse

In order to investigate the stability and reusability of catalyst, five successive RB 19 degradation cycles were performed. Reusability experimentswere conducted under the following conditions 25 mg dm^{-3} RB 19, 500 mg dm^{-3} C-BONH for a period of 150 min. The catalyst was separated by centrifugation at 3000 rpm for 5 min and concentration of RB 19 was determined in filtrate. After that catalyst was rinsed with DI-water for 5 times and dried overnight using an oven at 80ºC before bein re-using for the following cycle of RB 19 degradation.

3 Results and Discussion

3.1 Structure and physicochemical properties of C-BONH

FTIR studies were done to obtain information about the functional groups specific for C-BONH. The FTIR spectrum of the photocatalyst is given in Fig. 1. The spectrum of this powder shows a broad absorption band at 3536 cm^{-1}, which correspond to the stretching modes of hydroxyl groups and lattice water. The bands around 2360–2337 cm^{-1} were assigned to the asymmetric stretching of CO_2 molecules adsorbed on the surfaces and at 1553 cm^{-1} that were ascribed to the bending vibration of physisorbed water molecules[15–17]. The absorption bands at 1455–1349cm^{-1} were attributed to the deformation vibration of OH in plane. The characteristic IR peaks below 1000 cm^{-1} were very important to study the presence or absence of metal-oxygen bonds[18,19]. FTIR spectra exhibited strong vibrations around 812, 570, 467 and 429 cm^{-1} which could be assigned to the stretchingvibrations of metal-oxygen bond[20,21]. Based on all the above bands, FTIR spectra confirmed the formation of novel CuO/Bi oxide nitrate hydroxide hydrate structure.

The morphology and size of the sample werestudied by SEM. It could be seen that C-BONH photocatalyst is composed of two and three-dimensional sheet-like nanostructures with uniform thickness of about 200 nm and relatively smooth surface (Fig. 2 (a & b)). This implies that the C-BONH photocatalyst has a relatively large surface areaimportant characteristic for the photocatalytic activity. In addition, the component of C-BONH photocatalyst was further investigated by EDS. The EDS spectrum and the quantitative elemental composition were shown in Fig. 2c. It was concluded that C-BONH photocatalyst was composed of Bi, Cu, O and N elements.

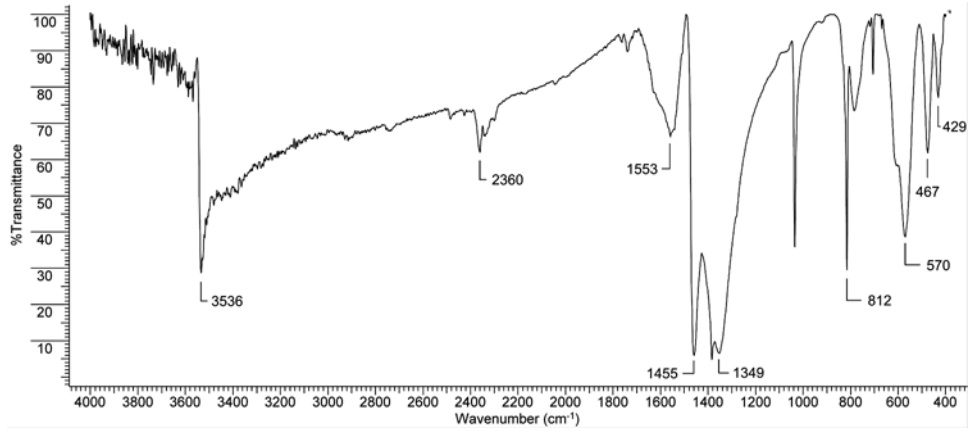

Fig. 1 — FTIR spectrum of C-BONH photocatalyst.

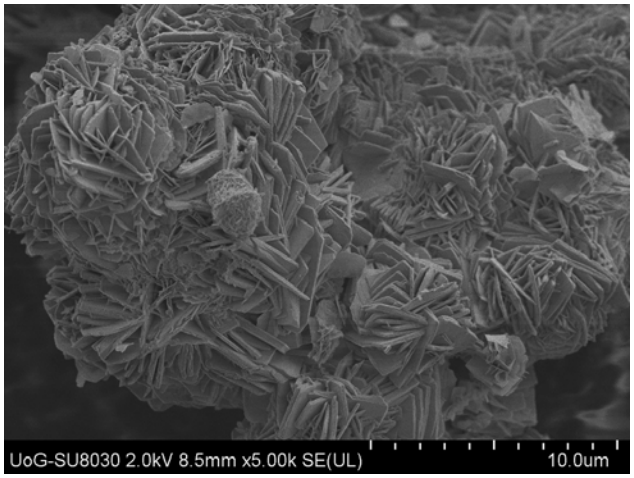

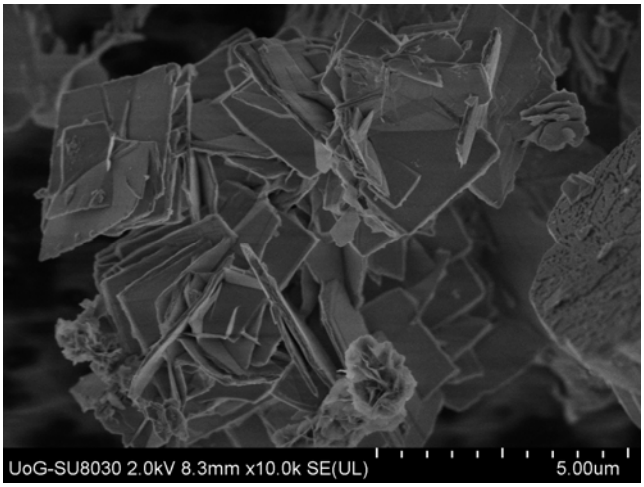

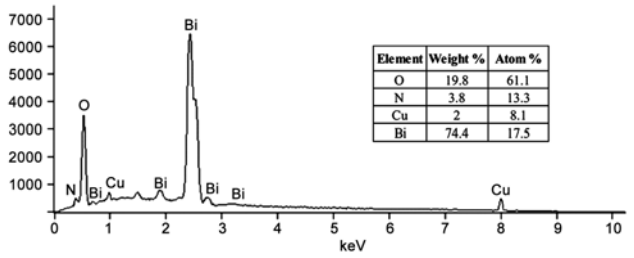

Fig. 2 — (a) SEM images of C-BONH photocatalyst and (b) SEM images of C-BONH photocatalyst at different magnification and (c) EDS spectrum of C-BONHphotocatalyst.

The XRD pattern of prepared powder is given in Fig. 3. All the observed peaks of the pattern can be indexing to a pure tetragonal $Bi_6O_6(OH)_3(NO_3)_3 \cdot 1.5\ H_2O$, that exhibits diffraction maxima with the values equal to 10.34º, 20.76º, 25.56º, 31.38º and 42.18º as Xie, Wang, Hu, Zheng *et al.*[12] and Xie, Wang, Hu, Zhu *et al.*[22] reported. The distinct peaks at 10.34º, 20.76º, 25.56º, 31.38º and 42.18º match with the (002), (004), (102), (006), (008) crystal planes of $Bi_6O_6(OH)_3(NO_3)_3 \cdot 1.5\ H_2O$, respectively. As seen

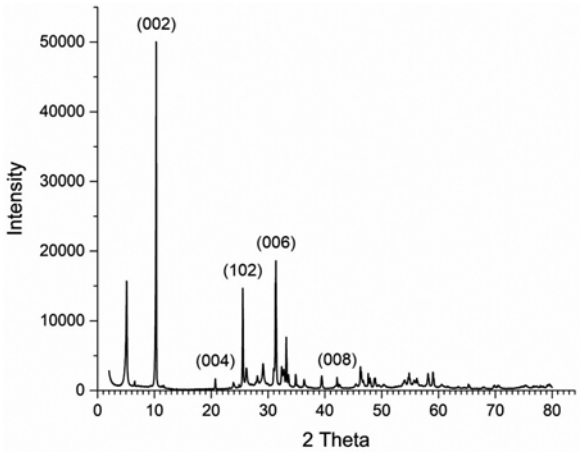

Fig. 3 — XRD pattern of C-BONHphotocatalyst.

in Fig. 3, no peaks for CuO were observed. This phenomenon may be attributed to the much lower diffraction intensity of CuO then that of $Bi_6O_6(OH)_3(NO_3)_3 \cdot 1.5\ H_2O$.

The specific surfacearea (SSA) was estimated using the BET method. The N_2 adsorption/ desorption isotherm of C-BONH are classified as a type IV, with mesoporous nature according to the IUPAC classification[23,24]. The obtained SSA using BET method is 4.42 $m^2\ g^{-1}$ which is similar to other bismuth-based photocatalyst reported in literature[5,6,9,12,25–27]. The BJH method reveals that photocatalyst is mainly composed of mesoporous, presence of which has significant influence on enhanced photocatalytic performance of material. The BJH surface area of pores is 4.39 $m^2\ g^{-1}$, and volume of pores is 0.0175 $cm^3\ g^{-1}$. The average pore diameter is 16.03 nm. The additional information regarding BET results is presented in Fig. S2 in Supplementary material section.

3.2 Photocatalytic studies

Photodecolorization process assisted by photocatalyst dependson various parameters like concentration of organic pollutant, concentration and type of photocatalyst, pH, *etc.* Different experiments were done to determine the photocatalytic performance of C-BONH photocatalyst.

3.2.1 Effect of the initial dye concentration on the photocatalytic performance

The effect of initial dye concentration on the decolorization efficiency was investigated by varying its value from 10 to 100 mg dm^{-3} at constant catalyst loading and pH value of the solution. The results are shown in Fig. 4a. As shown, the decolorization efficiency decreases with increasing dye concentration.

At higher dye concentrations, production of hydroxyl and superoxide radicals is reduced due to adsorption of dye molecules on the active sites of the photocatalyst surface. Also, as the dye concentration increases, the solution becomes less transparent to UV light because dye molecules may absorb a significant amount of UV light. Thus, the path length of photons entering the solution decreases and less number of photons is available to reach the photocatalyst surface[28].

3.2.2 Effect of photocatalyst dose on the photocatalytic performance

To determine the optimal photocatalyst dose, a series of experiments were conducted by varying the initial photocatalyst dose (20, 100, 500, 1000, and 2000 mg dm^{-3}) at native pH and fixed initial dye concentration. The results are shown in Fig. 4b. An increase in photocatalyst dose from 20 to 2000 mg dm^{-3} increases the decolorization rate rapidly. The total active surface area increases with the increasing of photocatalyst dosage, hence decolorization is faster[29]. Due to the large increase in the catalyst concentration, there is no consequential change in removal efficiency. Thus, it can be concluded that higher photocatalyst dose may not be useful. Hence, the optimal photocatalyst concentration is 500 mg dm^{-3}.

3.2.3 Effect of the initial pH on the photocatalytic performance

The photocatalytic activity was investigated at various initial pH values (2, 3, 5, 7 and 11), using fixed dye concentration and photocatalyst dose. The decolorization of dye as a function of the initial pH is shown in Fig. 4c. It can be observed that decolorization efficiency is the largest in acidic medium (pH 2). With the increase of initial pH from 2 to 11, decolorization efficiency decreases. The decolorization efficiency slightly decreases between initial pH 2 and 3. Such a dependence of pH on the decolorization efficiency can be explained by the dye adsorption capability of photocatalyst at the different pH values. To study this effect, dye adsorption on the photocatalyst surface was investigated at different pH values (results not shown). Adsorption was negligible at the pH 3, while it is significantly higher at pH 2 (about 6 mg g^{-3}). This can be explained by the surface charge according to pI value. At pH 2, photocatalyst surface is positively charged (pI is 3.54) and, because RB19 is anionic dye and thus negatively charged, the adsorption at pH 3 is favoured because of the electrostatic attraction between the dye molecules and photocatalyst surface. Thus, the decolorization efficiency is highest at low pH values, because electrostatic attraction and sorption of RB19 accelerate the photocatalytic process.

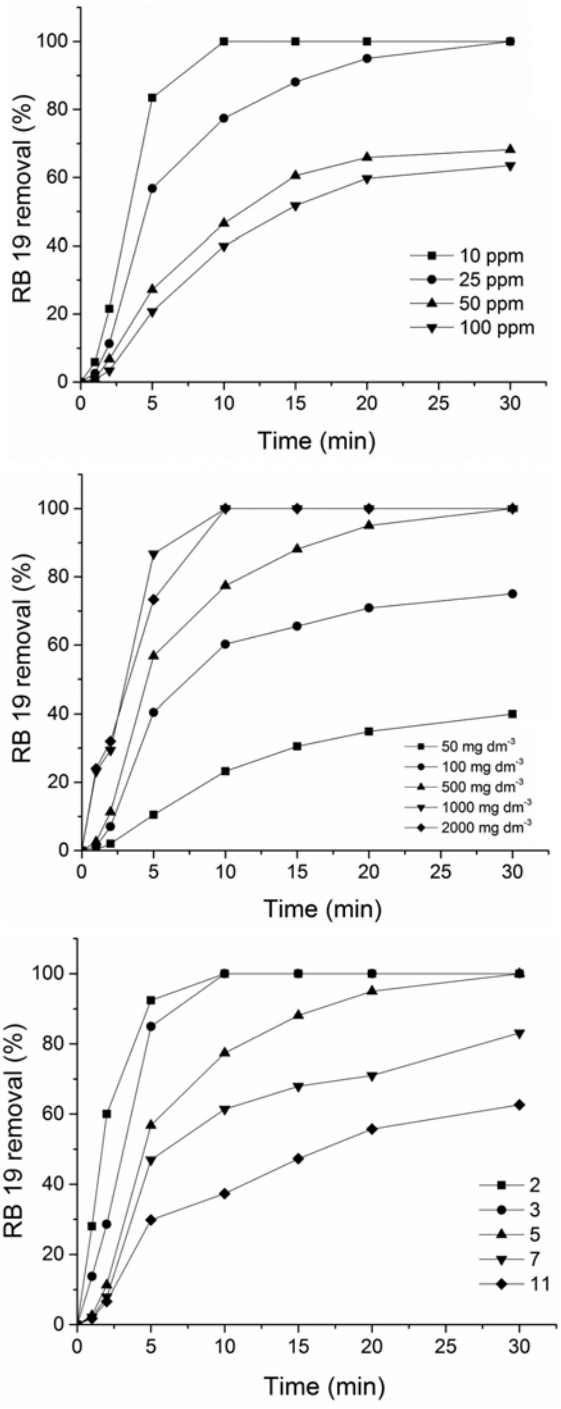

Fig. 4 — (a) Effect of initial dye concentration ($c_{photocatalyst}$ 500 mg dm^{-3}), (b) effect of photocatalyst dose (c_{RB19} 25 mg dm^{-3}), and (c) effect of pH (c_{RB19} 25 mg dm^{-3},$c_{photocatalyst}$ 500 mg dm^{-3}) on RB 19 removal efficiency. UV light intensity 1950 μW cm^{-2}, temperature 25 ± 0.5ºC.

The results show that C-BONH has higher photocatalytic activity than the photocatalysts based on bismuth compounds reported in other researches. For example, Li *et al.*[5] studied the photocatalytic activity of Dy doped Bi_2O_3 and results showed that 31.5% MO dye was removed for 60 min with dye/catalyst ratio $3.05 \cdot 10^{-5}$ mol mg^{-1}. Xie, Wang, Hu, Zheng *et al.*[12] also examined the removal of MO dye, but also MG dye, with the use of a $Bi_6O_6(OH)_3(NO_3)_3 \cdot 1.5H_2O$ photocatalyst. With dye/catalyst ratio $6.11 \cdot 10^{-5}$ and $5.48 \cdot 10^{-5}$ mol mg^{-1} the removal efficiency was 96.0% (40 min) and 74.0% (120 min) for MO and MG, respectively. Enhanced photocatalytic performance of Bi_2O_3/H-ZSM-5 composite for RhB dye was studied by Wang *et al.*[30]. They got to be removed 95.0% dye in 120 min (dye/catalyst ratio $1.04 \cdot 10^{-5}$ mol mg^{-1}). In this work C-BONH photocatalyst removed 90.3% of RB 19 dye for 15 min of treatment, with dye/catalyst ratio $7.98 \cdot 10^{-5}$ mol mg^{-1}.

For the improvement of photocatalytic performance, there may be several factors listed below. Firstly, the specific surface area is always an important influencing factor in photocatalysis[22]. Significantly higher surface area and pore volume of CuO/Bi oxide nitrate hydroxide hydrate (C-BONH) contributed to higher photocatalytic activity.

In general, photocatalytic degradation of the dye molecules began with the generation of photoinduced electron–hole pairs under the light irradiation. Then the electron–hole pairs were separated and subsequently migrated to the surface of the photocatalyst. During this process, several reactive intermediate species were generated such as h^+, •OH, and $•O_2^-$. The composites with small energy gap are more easily excited by UV light with both short and long wavelength to generate electrons and holes[31–33]. These more electrons and holes can lead to the formation of more reactive radicals (•OH, and $•O_2^-$). This may be the explanation why the catalyst obtained in this paper is more efficient than those mentioned in the literature.

3.3 Kinetics

Different types of kinetic models for the heterogeneous photocatalytic process were studied. Herein, to model the process we evaluated the kinetics of RB 19 decolorizationusing four models: Langmuir–Hinshelwood model (L–H)[34,35], pseudo-first-order kinetic model, pseudo-second-order kinetic model[36] and Chrastil model[37]. The equations, parameters were determined by nonlinear fitting of the experimental data for different initial concentrations of the dye and results are presented in Table 1.

As shown by Thu and Juang[35] for low substrate concentrations (approximately < 10^{-3} mol dm^{-3}) and when adsorption is relatively weak, L–H equation can be simplified to a pseudo-first order relationship. As shown in Table 1, the determination coefficients are high for all initial concentrations of dye and can be concluded that the photocatalytic process follows the pseudo-first order kinetics model.

At the investigated concentrations the applicability of L–H equation for the photocatalytic degradation was confirmed by the linear plot (Fig. S3 in Supplementary material section) obtained by plotting the reciprocal of reaction rate ($1/r$) against reciprocal of the initial concentration of RB 19 ($1/c_0$).The values

Table 1 — Kinetic parameters for photocatalytic decolorization of RB 19.

Model	parameter	c_{RB19} 10 mg dm^{-3}	c_{RB19} 25 mg dm^{-3}	c_{RB19} 50 mg dm^{-3}	c_{RB19} 100 mg dm^{-3}
	$q_{exp\ (mg\ g^{-1})}$	19.91	49.85	88.23	149.35
Langmuir–Hinshelwood	$k_{app\ (min^{-1})}$	0.41	0.24	0.18	0.08
	R^2	0.970	0.969	0.986	0.982
Pseudo-first	$q_{e\ (mg\ g^{-1})}$	20.77	52.23	89.44	149.98
	$k_{1\ (min^{-1})}$	0.51	0.29	0.22	0.12
	R^2	0.993	0.992	0.995	0.993
Pseudo-second	$q_{e\ (mg\ g^{-1})}$	25.42	69.52	108.39	198.12
	$k_{2\ (g\ mg^{-1}\ min^{-1})}$	0.69	0.33	0.25	0.11
	R^2	0.951	0.970	0.978	0.985
Chrastil	$q_{e\ (mg\ g^{-1})}$	19.90	48.16	88.20	146.74
	$k_{c\ (dm^{-3}\ mg^{-1}\ min^{-1})}$	1.29	0.46	0.34	0.26
	n	0.89	1.08	1.02	1.01
	R^2	0.984	0.989	0.991	0.985

for the equilibrium constant for adsorption (K) and the reaction rate constant (k_r) were found to be 0.09 dm^{-3} min^{-1} and 11.11 mg dm^{-3} min^{-1}, respectively. Determination coefficient R^2 is 0.995. Because the reaction rate constant of the photocatalytic reaction is large, and the adsorption constant is small, adsorption is a limiting factor of the photocatalytic reaction and thus sorption kinetics models can be applied on this process.

The data for the photodegradation of RB 19 on the photocatalyst was applied to pseudo-first and second-order kinetic model for all initial concentrations of dye, and the results are presented in Table 1. The determination coefficients are slightly higher for the pseudo-first-order model and calculated q_e values from the pseudo-first-order model are in better agreement with experimental ones (Table 1). Therefore, it can be concluded that the photocatalytic process follows the pseudo-first-order kinetics model.

The Chrastil diffusion model is used for the description of the kinetics of the systems limited by diffusion. The parameters of the model: q_e, k_C and n, were determined by non-linear regression analysis of the experimental data for different initial concentrations of dye from 10 up to 100 mg dm^{-3},and results are presented in Table 1.In observed systemconstant n is approximately 1, which means that diffusion resistance is small and reaction follows the pseudo-first-order kinetics. Theoretically, calculated q_e values by this model are close to experimental values.The results obtained by the Chrastil model are in good agreement with the L–H model for the reaction with the pseudo-first-order kinetics.

3.4 Determination of COD

The chemical oxygen demand (COD) test is widely used as an effective technique to measure the organic strength of wastewater. The test includes the measurement of waste in terms of the total quantity of oxygen required for the oxidation of organic matter to CO_2 and water. The COD of dye molecule before and after the treatment was estimated under optimum reactions condition (c_{RB19} 25 mg dm^{-3},$c_{photocatalyst}$ 500 mg dm^{-3}, pH native). It is evident from Fig. 5 that the solution obtained after photodegradation showed a significant decrease in COD after 180 min treatment *i.e.* after photodegradation COD was decreased from 28.10 to 6.82 mg dm^{-3}. It is clear that the decreasing of COD is lower than the decolorization efficiency within the studied reaction period.

3.5 Catalytic stability ofC-BONH

In order to evaluate the potential applications in wastewater treatment of C-BONH, its cycling photocatalytic performance was also investigated using RB 19 as a pollutant. It is found that the removal of RB 19 reaches 87.02% after the fifth reuse, which is slightly lower than that of first using (100%) (Fig. 6).

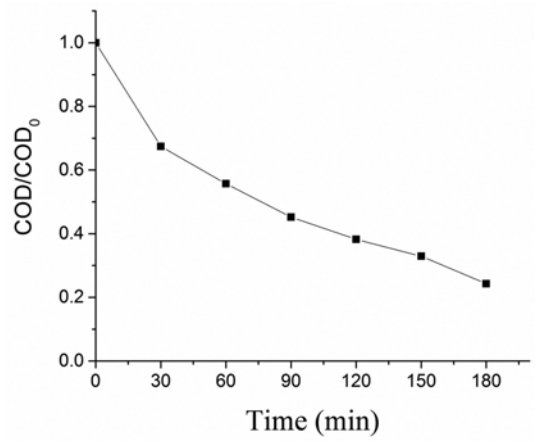

Fig. 5 — COD versus time plot for photodegradation of RB 19.

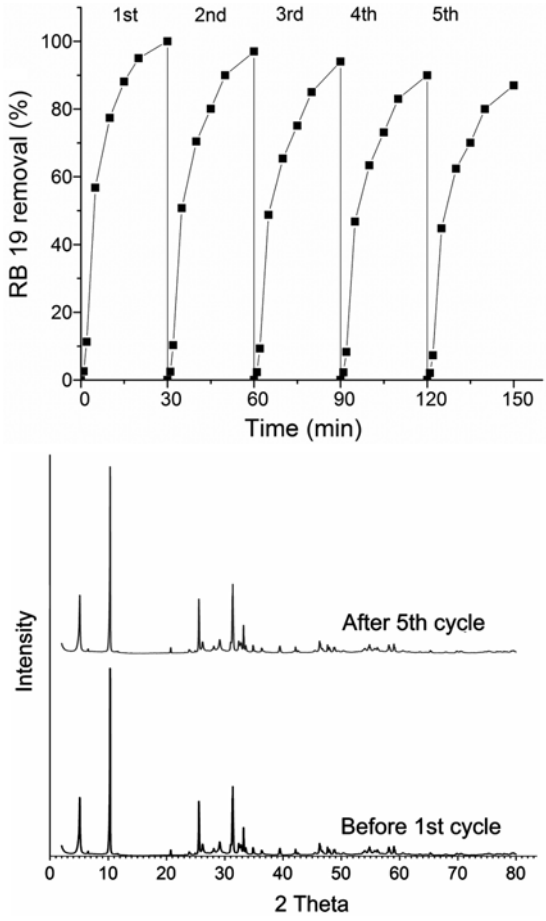

Fig. 6 — (a) Study on RB 19 removal efficiency in five successive cycles and (b) XRD patterns of C-BONH before first and after fifth cycle.

4 Conclusions

Novel photocatalyst CuO/Bi oxide nitrate hydroxide hydrate with sheet-like morphology can be synthesized by a simple hydrothermal method. The photocatalyst has been successfully characterized by FTIR, SEM, EDS,XRD and BET techniques. A relatively high surface area (4.42 m^2 g^{-1}) and mesoporous structure of material results with the high photocatalytic efficiency for decolorization of RB19.Under optimal conditions, total decolorization was achieved in less than 15minutes.The COD of dye solution decrease for more than four times after 180 min of the treatment.The photocatalytic process follows L–H model simplified to the pseudo-first-order kinetic model. From the Chrastil model it can be seen that diffusion has no influence on the photocatalysis process.

Due to facile synthesis, high efficiency, good reusability, low cost and eco-friendly starting materials, the nanosheet photocatalyst may be promising materials for photocatalytic degradation of organic pollutants. We expect that this investigation will be expanded with efficient photocatalytic degradation of pollutants using visible and UV-A light.

Acknowledgments

The authors would like to acknowledge financial support from the Ministry of Education, Science and Technological Development of the Republic of Serbia (Agreement No 451-03-68/2020-14/200124).

References

1 Rivera-Utrilla J, Gómez-Pacheco C V, Sánchez-Polo M, López-Peñalver J J & Ocampo-Pérez R, *J Environ Manag*, 131 (2013)16.
2 Wang S, *Dyes Pigments,* 76 (2008) 33.
3 Chen C, Ma W & Zhao J, *Chem Soc Rev,* 39 (2010) 4206.
4 Chong M N, Jin B, Chow C W K & Saint C, *Water Res*, 44 (2010) 2997.
5 LiJ Z, Zhon J B, Zeng J, Feng F M & HeJ J, *Mater Sci Semicond Process*, 16 (2013) 379.
6 Li K -L, Lee W- W, Lu C- S, Dai Y –M , Chou S -Y, Chen H -L, Lin H –P & Chen C –C, *J Taiwan Inst Chem Eng*, 45 (2014) 2688.
7 Liang L, Cao J, Lin H, Guo X, Zhang M & Chen S, *Mate Res Bull*, 80 (2016) 329.
8 SaisonT, Chemin N, Chaneac C, Durupthy O, Ruaux V, Mariey L, Mauge F, Beaunier P & Jolivet J –P, *J Phys Chem C*, 115 (13) (2011) 5657.
9 Shang M, WangW, Zhang L, Sun S, Wang L & Zhou L, *J Phys Chem C*, 113 (2009) 14727.
10 Wang K, Shao C, Li X, Miao F & Lu N, *J Sol-Gel Sci Technol*, 80 (2016) 783.
11 WuY C, ChaingY C, HuangC Y, Wang S F & Yang H Y, *Dyes Pigments*, 98 (2013) 25.
12 Xie L, Wang J, Hu Y, Zheng Z, Weng S, Liu P, Shi X & Wang D, *Mater Chem Phys*, 136 (2012) 309.
13 Brunauer S, Emmett P H & Teller E, *J Am Chem Soc*, 6(1938) 309.
14 Barrett E P, Joyner L G & Halenda P P, *J Am Chem Soc*, 7 (1951) 373.
15 Bagwasi S, Niu Y, Nasir M, Tian B & Zhang J, *Appl Surf Sci*, 264 (2013) 139.
16 Chang C, Zhu L, Fu Y & Chu X, *Chem Eng J*, 233 (2013) 305.
17 Vasantharani P & Sankeeda I, *Int J Recent Sci*, 4 (2013) 61.
18 Prekajski M, Kremenovic A, Babic B, Rosic M, Matovic B, Radosavljevic-Mihajlovic A & Radovic M, *Mater Lett*, 64 (2010) 2247.
19 Kumar A M & Muthukumaran S, *J Alloys Compd*, 587 (2014) 606.
20 Li N, Yang B, Xu L, Xu G, Sun W & Yu S, *Ceram Int*, 42 (2016) 5979.
21 Chae B W, Amna T, Hassan M S, Al-Deyab S S & Khil M S, *Adv Powder Technol*, 28 (2017) 230.
22 Xie L, Wang J, Hu Y, Zhu S, Zheng Z, Weng S & Liu P, *RSC Adv*, 2 (2012) 9881.
23 Sing K S W, Everett D H, Hau R A W, Moscou L, Pierotti R A, Rouquerol J & Siemieniewska T, *Pure Appl Chem*, 57 (1985) 603.
24 Yu H G, Liu R, Wang X F, Wang P & Yu J G, *Appl Catal B Environ*, 111–112 (2012) 326.
25 Anandan S, Lee G -J, Chen P -K, Fan C & Wu J J, *Ind Eng Chem Res*, 49 (2010) 9729.
26 Irmawati R, Nasriah M N N, Taufiq-Yap Y H & HamidS B A, *Catal Today*, 93–95 (2004) 701.
27 LiuS, Tu Y & Dai G,*Ceram Int*, 40 (2014) 2343.
28 Byrappa K, Subramani A K, Ananda S, Rai K M L, Dinesh R & Yoshimura M, *Bull Mat Sci*, 29 (2006) 433.
29 Daneshvar N, Salari D & Khataee A, *J Photochem Photobiol A Chem*, 162 (2004) 317.
30 Wang Q, Hui J, Yang L, Huang H, Cai Y, Yin S & Ding Y, *Appl Surf Sci*, 289 (2014) 224.
31 Cao C, Xiao L, Chen C & Cao Q, *Appl Surf Sci*, 357 (2015) 1171.
32 Labib S, Saudi J, *Chem Soc,* 21 (2017) 664.
33 Luo Y, Huang Q, Li B, Dong L, Fan M & Zhang F, *Appl Surf Sci*, 357 (2015) 1072.
34 Hamad H A, Sadik WA, El-latif M M A, Kashyout A B & Feteha M Y, *J Environ Sci*, 43 (2016) 26.
35 Thu A & Juang R, *J Environ Manage*, 147 (2015)271.
36 Azizian S, *J Colloid Interface Sci*, 276 (2004) 47.
37 Chrastil J, *Text Res J*, 60 (1990) 413.